minimum number of animals, or even samples of in vitro-cultured cells after a relatively short period of exposure to a potential hazardous testing materials. The predictability by reverse toxicology depends upon the number of gene expression profiles accumulated, the number of phenotypes differentially linked to the gene expression profiles, and informatics linking such gene expressions and the phenotypes.

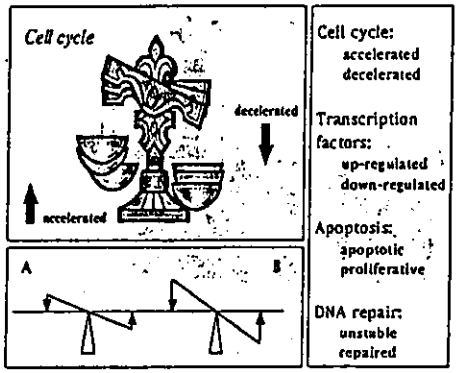

Fig. 3. Counter balancing gene expressions behind the homeostasis Visualization of different oscillatory balances A and B (left bottom).

At this moment, reverse toxicogenomics is still a theory. However, a variety of testing methods in toxicology will be replaced by reverse toxicogenomics, eventually. This strategy has the following advantages: it reduces the number of test animals, and the test period, and adopts simpler techniques by using established expression profile as new biomarkers rather than sophisticated methodologies requiring skill and experience. Furthermore, a specific proteome chip, expressing a series of specific genes, is supposed to function as "reverse proteomics" through a series of processes such as sample preparation, 2D gel electrophoresis, and mass-spectrometry for image analysis (Zhu et al., 2001). To set up an endpoint where NOEL or NOAEL exists, a traditional toxicology has been applied to incorporate something " invisible borders". Invisible borders are, in conventional toxicology, based on at least two major limitations: one in an endogenous factor(s) and the other in an exogenous factor. The former, for example, is hidden behind homeostasis, and the latter, for example, is behinbd a technological limitation. As shown in **Figure 3**, most living animals exhibit homeostasis between two (or more) counter- balancing vectors such as oxidation & reduction, apoptosis & anti-apoptosis, and acceleration & deceleration of cell cycle regulation. Since the counter-balancing counter-directional homeostasis, it appears static and one may not recognize the differences between one homeostatic stage, balanced at a low energy stage, to the other stage, balanced at a high energy stage (A and B in Figure 3). It is far more important to note that stage B is generally more risky. Toxicogenomics is expected to disclose such hidden homeostatic balances which are undetectable by conventional testing systems. The latter, an exogenous factor in a technological limitation, may be based on such resolution limit of light-microscopes, spectrophotometers, etc., and all

messenger RNAs are extracted, and visualized with red color marker, cy3, for overexpression or with green color marker, cy5, for down-modulation. These color-labeled mRNAs will be processed into a competitive mixed-hybridization in a high-density hybridization array. Expression patterns are informatized in many ways. Along with accumulation of data to establish informatic profiles, specific gene clusters for TRC, NTRC, and those positive for both TRC + NTRC, andnegative for both TRC + NTRC, can be established. These databases can be compared with an expression profile that will be obtained from unknown chemicals (left box in Figure 4).

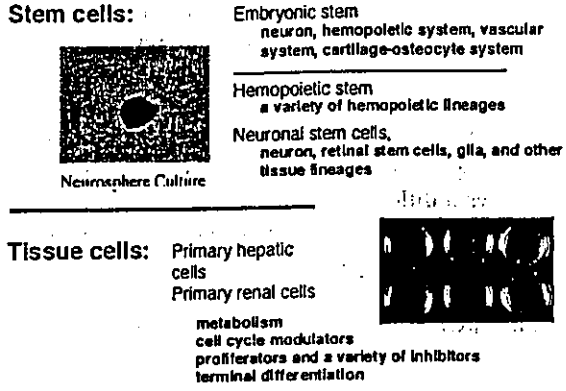

Fig. 5. A variety of in vitro resources for toxicologic gene expression array. Different cellular function for microarray analyses between stem cells and tissue cells. See text.

The technique requires only a limited number of animals, or even with cultured cells, in vitro, after relatively a short period of exposure. Depending upon the endpoints of toxicity aimed to focus on, even materials from in vitro culture may work efficiently (**Table 1**). As shown in Table 1, activities of membrane such as ion channels and ion pumps, the inhibitory effect of uncoupling oxidative phosphorylation, and the inhibition of ATP turnover by redox cycling, may be identified by the microarray. Possible toxicity related to developmental anomaly and morphogenesis (top of Table 1) may not be predictable by the use of in vitro cell culture; however, as seen in **Figure 5**, an in vitro system, for example, an embryonic stem (ES) cell, may predict some possible adverse effects of toxicity on the morphogenesis. Consequently, ES cells as well as hemopoietic and neuronal stem cells are particularly powerful tools for identifying the effect of toxicity on not only proliferation but also differentiation. Actually, one ES cell potentially corresponds to one individual; therefore, observing a microarray of ES cells may correspond to observing several millions of mice at the early developmental stage. Hepatic, renal and other types of primary cultured cells are limited but useful for observing such a variety of metabolic modulators, cell cycle regulators, and cell proliferation inhibitors and/or stimulators, in primary hepatic cells.

Reverse toxicology as a future predictive toxicology

Jun Kanno

Cellular and Molecular Toxicology Division, Biological Safety Research Center, National Institute of Health Sciences

Summary. The whole genome sequence of humans and rodents, and technical capability of monitoring the whole genome expression are now in our hands. In theory, "whole genome profiling" is a way to reveal the molecular events taking place inside our body or in experimental animals. The major characteristic of the whole genome profiling is that it does not require overt phenotyping *per se*. In other words, it is possible to build up a gene expression database regardless of the presence or absence of the classical toxicological phenotypes. This phenotype-independent approach can be considered "reverse toxicology" in contrast to the traditional toxicology or "forward toxicology", a phenotype-dependent approach currently performed as a standard procedure. The future of predictive toxicology would be based on a well-balanced informatics system composed of both the reverse and forward toxicology. This approach is intended to clarify, 1) the molecular based mechanisms of species/strain differences that will allow more accurate extrapolation of animal model data to humans and 2) a toxicogenomics-based risk assessment strategy that doesn't overlook "unexpected toxicity". In conclusion, in the future, toxicology will be fully developed as a mechanism-based science through the process of disclosure of the "black box" of organisms by coordinated implementation of reverse toxicology and forward toxicology.

Key words. Whole genome sequencing, DNA microarray, comprehensive gene expression monitoring, reverse toxicology

Toxicology has been a science based on phenotypes induced by exogenous agents in an organism. Toxic symptoms are categorized and the causative agents are classified in a symptom-based fashion. When human data are not available, rodent models as surrogates have been used to collect phenotype data for human risk assessment. This approach has served us well for a long time with a series of well-considered strategies including a concept of "safety factors" or "uncertainty factors". This empirical and practical approach has been based on the scientific knowledge available (Fig 1). However, because the strategy has been dependent on measurable phenotypes, it has not always been perfect. One well-known

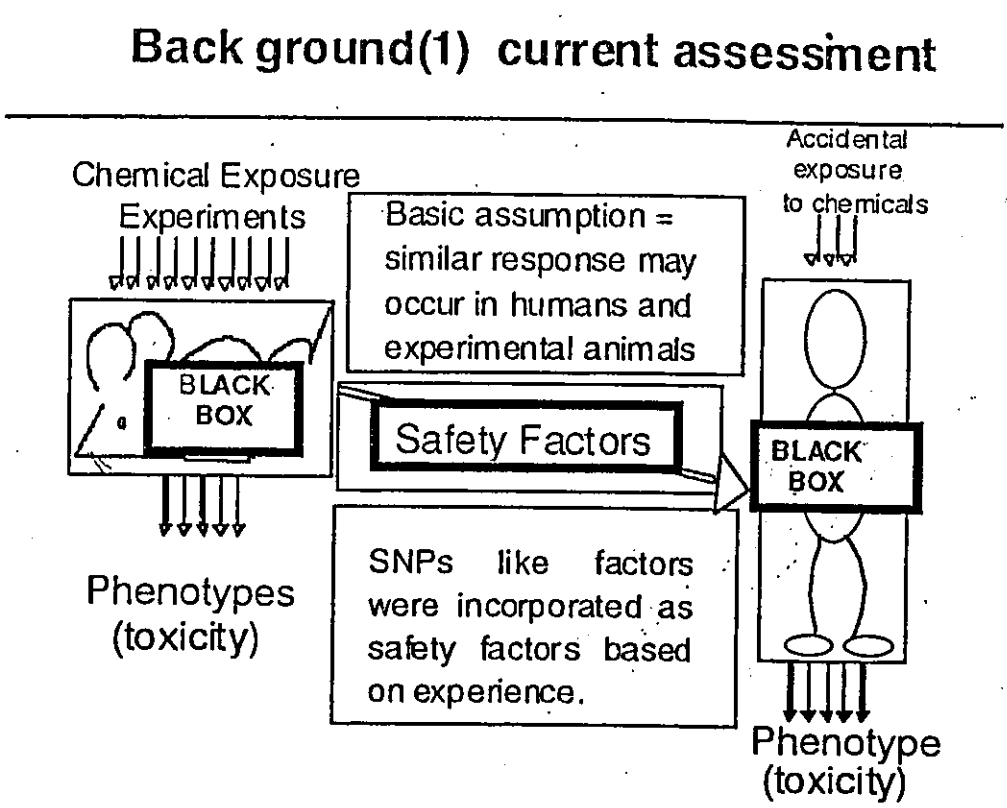

Fig. 1. The use of "Safety Factors" in traditional toxicology is based on available scientific knowledge of toxic phenotypes. This scheme has been robust as long as the black boxes are similar in quality in response to the xenobiotic challenges.

example is the thalidomide story, which induced no teratogenic responses in rat and mouse models, but did induce teratogenic effects in humans and rabbits. In order to improve the extrapolating process from rodents to humans, it is clear that a mechanism-based approach must be reinforced. Recent studies on thalidomide-regulated genes strongly suggest a possibility that teratogenic effects not observed in rodents can be monitored as angiogenesis-regulating properties even in the rodent models themselves (1,2). Once the responsible gene(s) or those closely related to a particular function/phenotype are identified in both species, extrapolation of the biological effects can be achieved with increased accuracy.

To identify responsible genes in mice, gene knockout (KO) technology can be applied, and in humans, single nucleotide polymorphism (SNPs) data can be utilized (Fig. 2). The limitation, however, is that these approaches are still phenotype-dependent. In other words, if there is no observable phenotype in a KO mouse, it is usually a "dead end" for further analysis on the function of the targeted gene. The same situation is usually true when the SNPs are not well

linked to a distinct symptom. Utilization of gene expression profiling by DNA microarray technique as a screening strategy is another way to identify mechanistically relevant genes. This approach is also dependent on phenotype and thus has the same limitation mentioned above.

To overcome the "dead end" situation in the case of "no observable phenotype", our proposal is to introduce a "reverse approach" paradigm. The approach is to construct a bioinformatics database dependent upon a gene expression profile generated even in the absence of a xenobiotics-induced phenotype. This approach is now possible because of two factors: 1) the

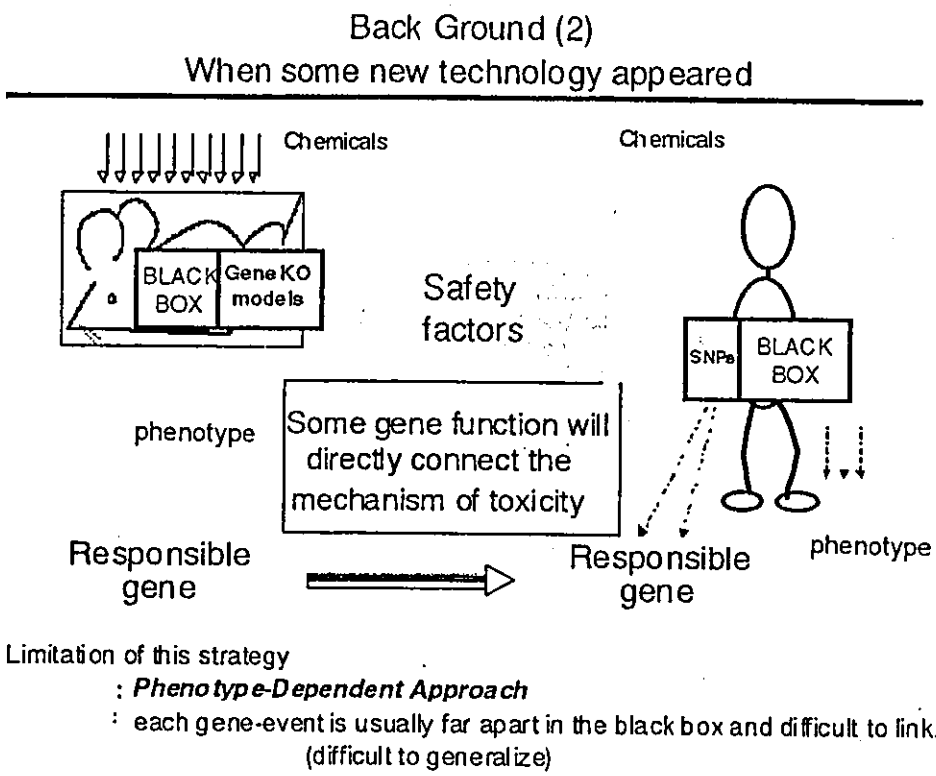

Fig. 2. Finding the responsible gene for a particular phenotype is possible by using gene knockout mice or SNPs (single nucleotide polymorphism) data in humans, as well as an attempt to screen out related genes by DNA microarray techniques. However, all these approaches are still dependent on phenotypes. If there is no phenotype in relation to treatment or genotype, the search for responsible gene usually becomes very inefficient.

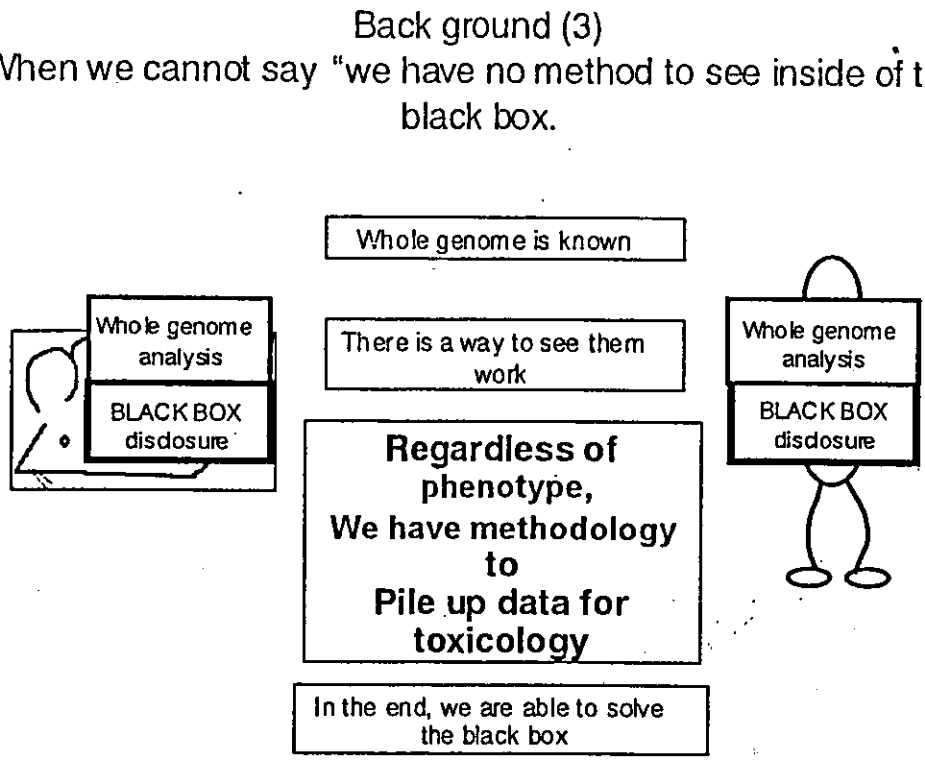

Fig. 3. When we know all genes, and know how to monitor their expression, it is theoretically possible to construct a database in a phenotype-independent approach that will eventually disclose the network inside the black box of our body.

availability of whole genome data, and 2) the availability of high throughput technology for comprehensive gene expression monitoring, i.e. the DNA microarray. We propose to first obtain whole genome expression data, and then to analyze what phenotype, if any, could be linked to the treatment-related gene expression profiles (Figure 3). This approach could be most effectively applied to the low dose issue in endocrine disruptor studies. In the endocrine system, exogenous perturbation is effectively cancelled out by homeostatic feedback mechanisms. Even though exogenous stimuli may fail to induce overt phenotype, such stimuli should clearly induce gene expression involved in a homeostatic response (Fig 4).

The DNA microarray technique is applicable to both a forward and reverse approach. In the forward approach, genes that are significantly altered in expression are linked to an overt phenotype. Databases built on such selected expression data are currently available and growing fast. In contrast, in the reverse approach, expression data on all genes, including those not linked to an observable phenotype, are equally important and incorporated into the database. To assure the quality of the database, strict normalization of gene expression levels is essential. In other words, unchanged gene expression should be monitored correctly as

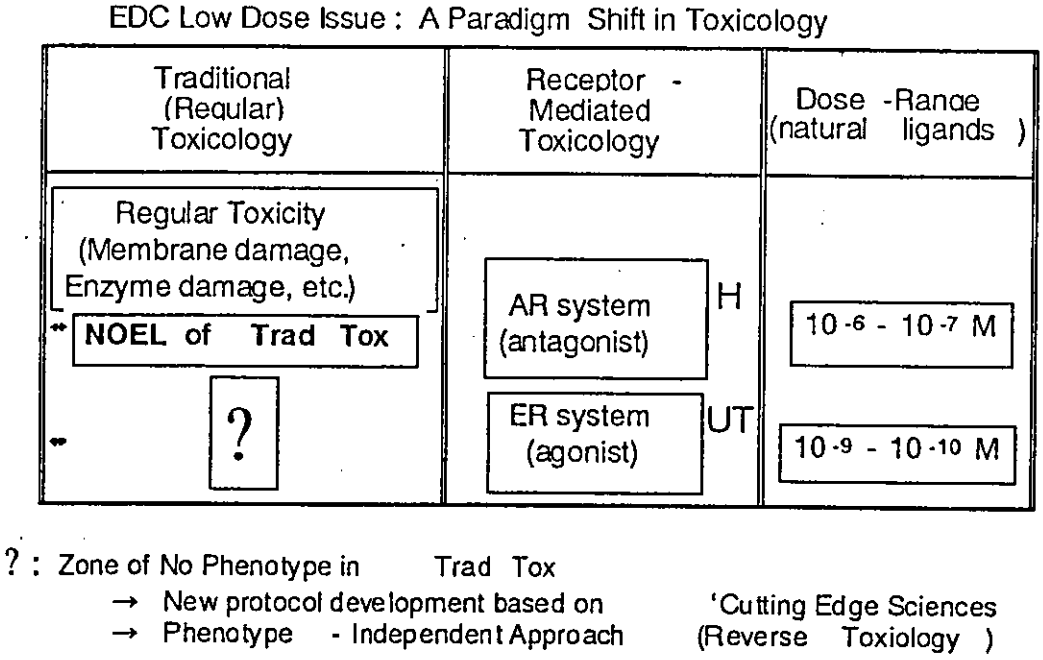

Fig. 4. The low dose issue of endocrine disrupting chemical research is the problem of gap between monitorable does-range in traditional toxicology and receptor mediated toxicology. Estrogenic responses monitorable, at least, by uterotrophic assay (UT) and some of the androgenic responses monitorable by Hershberger assay (H) are below the level of no observed effect level (NOEL) of traditional toxicology studies. The range indicated by "?" is the zone of no-phenotype in traditional toxicology. There seems to be two ways to handle this "?" zone, 1) develop new test protocols by cutting edge sciences, 2) apply reverse toxicology as phenotype-independent approach.

"unchanged". Reverse toxicogenomics requires continuity and compatibility of the data for its compilation. It includes a strategy to prepare a standard sample set to normalize various gene-expression monitoring platforms including SAGE, quantitative PCR, DNA microarray systems of different platforms, including different microarray versions in a particular system, different reading machines, and various microarray stocks, buffer stocks, etc.

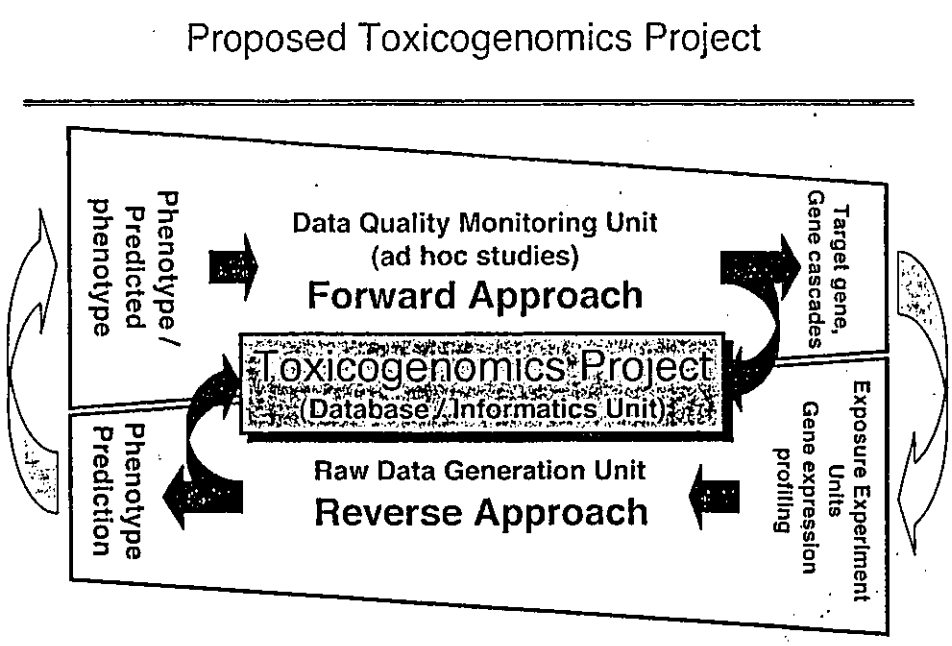

Fig. 5. Proposed Toxicogenomics Project is characterized by its components, the Reverse Approach and the Forward Approach. The database/informatics are built on data generated from both approaches.

The reverse approach will generate an enormous amount of raw data. A set of gene expression data that is linked to known phenotypes is essential for the startup of the toxicogenomics database. Then, gene clusters of unknown function will be investigated by a forward approach to connect the missing link to known gene clusters. This exploratory approach to functionally characterize unknown gene cluster demands ad hoc experiments including gene-knockout animal studies designed wisely by a multidisciplinary team of molecular biologists, chemists, toxicologists, pathologists, etc. (Fig 5.) The final goal is to fully develop a mechanism-based predictive toxicology through the process of disclosure of the "black box" of organisms by coordinated implementation of reverse toxicology and forward toxicology.

ANALYTICAL SCIENCES APRIL 2004, VOL. 20

The Best Paper in Bunseki Kagaku, 2002

Screening of Endocrine Disrupting Chemicals Using a Surface Plasmon Resonance Sensor

Kazunobu ASANO,† Atsushi ONO, Setsuko HASHIMOTO, Tohru INOUE, and Jun KANNO

New Business Development, Biacore K.K., Koyo Bldg. 5F, 2-9-5 Shiba Koen, Minato-ku, Tokyo 105-0011, Japan

Because concern over endocrine disrupting reactions caused by chemicals to humans and animals is growing, a rapid and reliable screening assay for endocrine disrupting chemicals is required. We have developed an *in vitro* screening assay based on a hormone receptor mechanism using a surface plasmon resonance (SPR) sensor. The interaction between an estrogen receptor α (ER) and an estrogen response element (ERE) is monitored in real time, when ER is injected over the SPR sensor chip on which a DNA fragment containing ERE is immobilized. In the presence of a chemical with estrogenic activity, the ER-ERE interaction is enhanced and the kinetic parameters are altered. We have validated the assay in terms of its specificity, dose dependency, optimal reaction conditions and reproducibility. It has been shown that the assay is very reliable as a rapid and quantitative screening method to judge the estrogenic activities of chemicals.

Introduction

Recently, concern has grown that some chemicals, such as organic chloride insecticides, plasticizers and detergents can cause endocrine disrupting effects to wild animals and humans.[1] Many of them are supposed to pose endocrine disrupting activities through direct interaction with the hormone receptors, such as estrogen receptor, thus modifying or inhibiting the physiological hormonal activities.[2] Chemical safety is evaluated by a set of the toxicological tests, such as carcinogenicity, teratogenicity, mutagenicity, reproduction tests. However, they have limitation to evaluate the chronic toxicity of chemicals. Moreover, the mechanisms of the endocrine disrupting activities are yet to be elucidated and the test methods to evaluate the effects are not well established.[3]

Several test methods have been reported to detect the endocrine disrupting activities caused by hormone receptors, *i.e.* competitive receptor binding assay, a cell growth assay using breast cancer cells expressing the estrogen receptors (MCF7),[4] cell-based reporter assay,[5] an *in vivo* rodent uterotrophic test,[6,7] and a vitellogenin assay using medaka fish (Oryzias latipes).[8] Many of these methods require a long time to obtain results. Furthermore, the endocrine disrupting activities can not always be detected when the chemicals are administered to the animals due to physiological regulations concerning the animal bodies. It is not easy to detect the hormonal effects of chemicals. The existing toxicological methods are not always the best way to detect the effects which have the feedback mechanism or the effects *via* the receptors. Therefore, a novel approach is sought for the rapid assessment of the endocrine disrupting activities of the chemicals.

The hormone receptors are the ligand dependent transcription factors. For example, estrogen receptor (ER) changes its conformation upon binding of the endogenous ligand, estrogen, and binds to the specific sequence of the DNA located upstream of the target genes and activates transcription of the genes (Fig. 1). Many chemicals with diverse structures have been reported to have estrogenic activities. Due to the variety of the structure, it is unlikely that all the chemicals act with the same mechanism. Each chemical may pose a different regulatory effect on the gene expression.[9]

Recently, a surface plasmon resonance (SPR) sensor is emerging as a novel analytical instrument.[10] The SPR sensor has features that it can monitor molecular interaction without labeling the molecules in real time. It is, therefore, suitable for high throughput screening assays. Compared to the existing technologies which monitor the binding amounts at the end of the interactions, the SPR sensor is unique to be able to detect the processes throughout the association and the dissociation of the interaction. This feature enables detailed analyses of chemical effects to receptors.

We have established a cell free screening assay focusing on the hormone receptor mechanism as a high throughput screening method for the endocrine disrupting chemicals. In order to measure the interaction of the biological molecules using the SPR sensor, one of the test molecules is immobilized

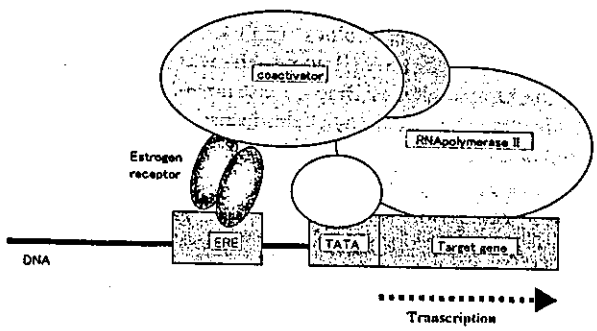

Fig. 1 Functional mechanism of the estrogen receptor in gene regulation.

† To whom correspondence should be addressed.

This is an English edition of the paper which won the Best Paper Award in Bunseki Kagaku, 2002 [*Bunseki Kagaku*, **2002**, *51(6)*, 389].

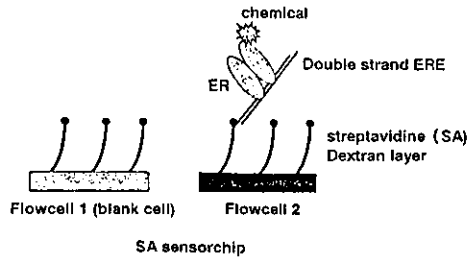

Fig. 2 Scheme of the ER-ERE assay with an SPR sensor.

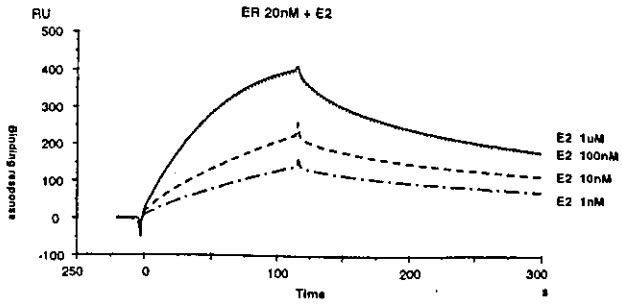

Fig. 3 Dose-dependent responses of E2.

on the sensor chip surface and a solution containing the other molecule is passed over the sensor surface at a constant flow rate through the microfluidics. A small mass changes, resulting from the binding and the dissociation of the two molecules on the sensor surface is monitored as SPR signals. The time course of the changes in the SPR signals is displayed as a curve called a sensorgram. Unlike from the conventional technologies, the SPR sensor can measure the interactions using a small amount of non-labeled samples within a short time. With regard to the interaction of the molecules, the SPR sensor can give not only the affinity of the two molecules at the equilibrium (as the dissociation constant, K_D or the affinity constant, K_A) but also the information on two molecules binding or dissociation velocity, namely the association rate constant (k_a) and the dissociation rate constant (k_d).

We have designed an assay to monitor the interaction of estrogen receptor α (ER) and the estrogen response element (ERE)[11] that is located in the promoter region of the estrogen target genes by immobilizing the DNA fragment containing the ERE sequence on the sensor chip and injecting purified ER over the sensor chip (Fig. 2). Thirty chemicals were tested for the estrogenic activities.

Experiments

Reagents and instruments

Reagent. Tricine, $CaCl_2$, $MgCl_2$, KOH, Tween 20, NaOH and HCl were purchased from Nacalai Tesque and DMSO from Sigma. Estrogen receptor (ER) was purchased from PanVera. ER was aliquoted into 5 µl and stored at –80°C. Biotinylated estrogen response element (ERE) DNA (5′-biotin-tcgagcaaagtcaggtcacagtgacctgatcaat-3′) of viterogenin gene and the anti-strand DNA have been synthesized by Nisshinbo. The synthesized oligomers were diluted with MilliQ water to 1 mg/ml and stored at –20°C. The running buffer for Biacore 3000 was prepared by filtering a solution of 25 mM Tricine, 160 mM KCl, 5 mM $MgCl_2$ (pH 7.8), 0.05% Tween 20.

Instrument. The assay was performed using Biacore 3000 (Biacore AB), the heat block (EYELA) and the circulator (Asone). Sensor chip SA (Biacore AB) was used. Through the assay, the sample rack of Biacore instrument was cooled to 4°C by connecting the circulator to the instrument and the reaction was run at 25°C.

Operation

Immobilization of biotinylated ERE. For the immobilization of biotinylated ERE to the sensor chip, a streptoavidin preimmobilized sensor chip (Sensor chip SA) was set to the Biacore 3000 instrument and the instrument was equilibrated with running buffer. In order to stabilize the sensor surfaces, 100 mM NaOH and 50 mM HCl were injected for 30, 5 times. After checking the baseline stability, we performed immobilization of the biotinylated ERE. Biotinylated ERE (1 mg/ml) was diluted hundred thousand times with the running buffer. Then, 100 µl of the ERE solution was heated in boiling water for 5 min and chilled rapidly to denature the biotinylated ERE. The solution was injected over the sensor surface to immobilize approximately 60 RU onto the SA sensor chip surface. Then, the complementary ERE (1 mg/ml) was diluted to 100 times with the running buffer and denatured by the same method. This solution was injected for 2 min over the sensor surface where the biotinylated ERE was immobilized to form double stranded ERE on the surface. Biotin (1 µg/ml) was injected to block free SA on the sensor surface. A separate flow cell was used as a blank cell on which only biotin was immobilized.

Preparation of the test chemicals. Each chemical was dissolved with 100% DMSO to make 0.1 M stock solution, and stored at –80°C. Immediately before the assay, 1 µl of the stock solution was diluted 500 times using the chilled running buffer. Also ER stock solution was diluted to 40 nM using a chilled running buffer. A 50-µl volume of the ER solution and 50 µl of the chemical solution of each concentration were mixed to give final concentrations of 20 nM ER and 10 µM to 1 nM of the chemical. The samples were kept at 4°C in a sample rack to maintain the ER activity. 17β-Estradiol was used as a positive control. First, we prepared the various concentration of 17β-estradiol (1 µM to 1 nM) and measured the binding of ER to ERE (Fig. 3). As the binding activity of ER to ERE was plataued over 100 nM 17β-estradiol, we decided to use 100 nM 17β-estradiol as a positive control in the following experiments. We also prepared a negative control solution which did not contain any chemicals. After the preparation of samples, the samples were treated at 37°C, 5 min and rapidly cooled. The samples were then set on the sample rack for measurements.

Assay of ER and ERE. The prepared samples were injected for 2 min at a flow rate of 20 µl/min over the immobilized ERE and the blank flowcell. Injection command of "kinject" was used and the dissociation phase was monitored for 2 min. The "kinject" command is one of the injection commands specially designed for the kinetic analysis in the Biacore instrument. Upon injecting the samples using "kinject" command, the sample solution was clearly separated by two air plugs at the both ends of the sample solution from the running buffer in order to prevent the sample solution from being diluted by the running buffer. The command is also designed to monitor dissociation of the bound molecule without being disturbed by the movement of the injection needle for the set period of time. After monitoring the binding and dissociation, 100 mM NaOH and 50 mM HCl were injected 30 s each for regeneration of the sensor surfaces. All the measurements were run automatically.

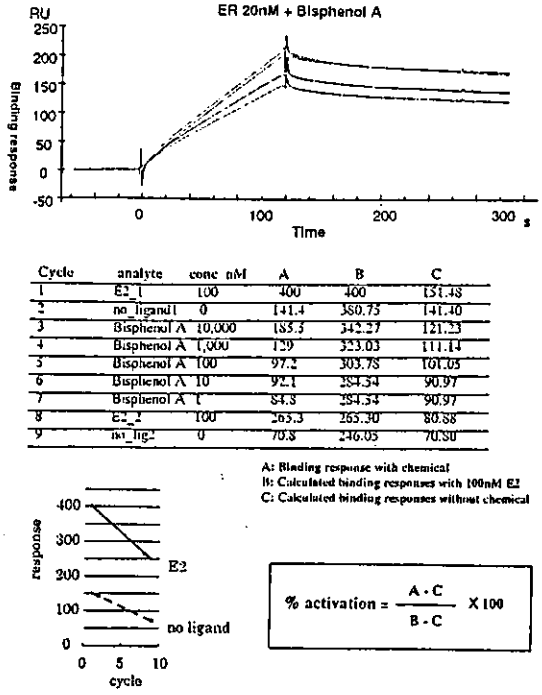

Cycle	analyte	conc nM	A	B	C
1	E2_1	100	400	400	151.48
2	no_ligand1	0	141.4	380.75	141.40
3	Bisphenol A	10,000	185.3	342.27	121.23
4	Bisphenol A	1,000	129	323.03	111.14
5	Bisphenol A	100	97.2	303.78	101.05
6	Bisphenol A	10	92.1	284.54	90.97
7	Bisphenol A	1	84.8	284.54	90.97
8	E2_2	100	265.3	265.30	80.88
9	no_lig2	0	70.8	246.05	70.80

A: Binding response with chemical
B: Calculated binding responses with 100nM E2
C: Calculated binding responses without chemical

$$\% \text{ activation} = \frac{A-C}{B-C} \times 100$$

Fig. 4 Data evaluation of chemical screening.

Data evaluation

A set of the assay consisted of 5 concentrations of the test chemical, a negative control (no chemical) and a positive control (100 nM 17β-estradiol). The results were compared as the ratio to the positive control (% activation). ER was unstable and lost its binding activity to ERE during the assay period in spite of optimizing the assay conditions. We have developed an assay design to correct for any loss of the binding activity of ER over time. A positive control cycle and a negative control cycle were run at the beginning and the end of the assay. The binding responses were recorded. Based on the rate of loss in the positive and negative control samples, the binding responses of the positive and negative controls for each cycle were calculated. The enhancement of ER binding by the test chemical was expressed as the ratio to those by the positive control of 100 nM 17β-estradiol, namely as a relative activation (% activation) using the formula and the corrected binding signals, as shown in Fig. 4.

Results

Validation of the ER-ERE assay using Biacore

In order to confirm the significance of the ER assay, the binding of ER to ERE was tested with a varying concentration of ER. The binding signals increased in relation to the increasing concentrations of ER. ER did not bind to the sensor surface where no ERE was immobilized (Fig. 5). A 1 μM volume of BSA did not show any significant binding to ERE surfaces (Fig. 6). These observations indicate that the assay monitors the specific binding of ER to ERE. Comparing the results with 10, 20 and 40 nM ER, we often observed relatively low binding signals with 10 nM ER. Higher binding signals were obtained by adding a final concentration of 1 μM BSA to 10 nM ER. Due to the low protein concentration, ER was lost by absorption to the surfaces of the plastic vials and tips and the actual concentration of ER became lower than 10 nM. Based on those results, we decided to run the following assays with the final ER concentration of 20 nM.

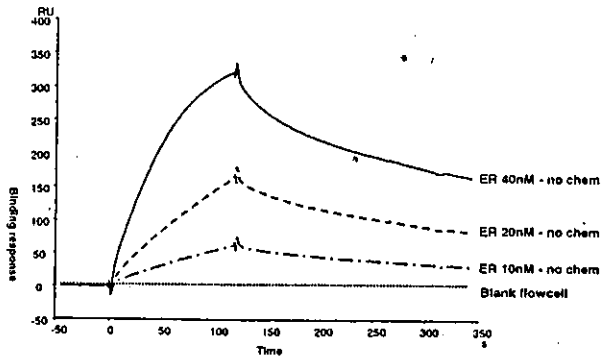

Fig. 5 Dose-dependent responses of ER-1.

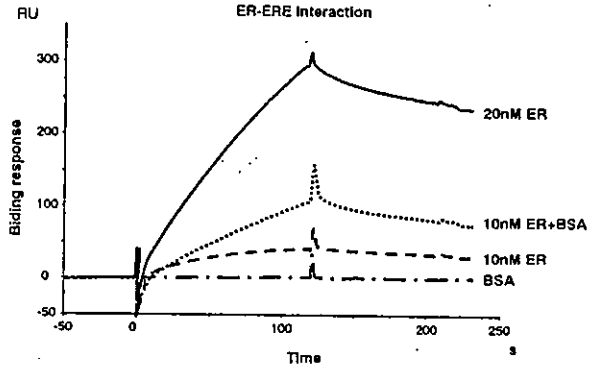

Fig. 6 Dose-dependent responses of ER-2.

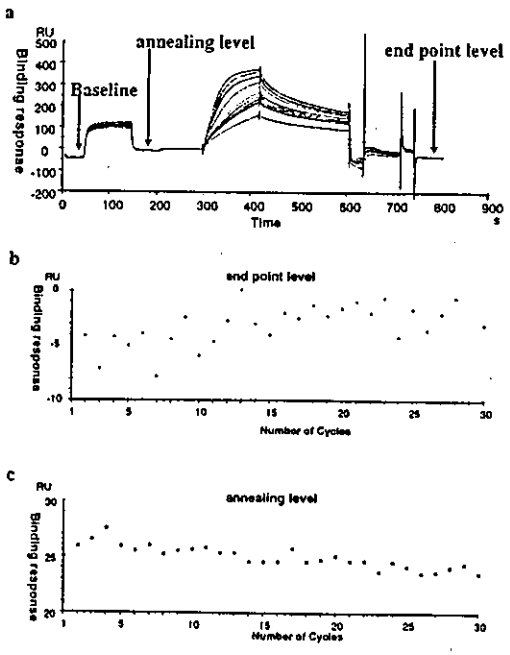

Fig. 7 Reproducibility of the ER-ERE assay.

It is important to regenerate the sensor surfaces to achieve reproducible results in the Biacore assay. We have repeated 30 cycles of the assay (Fig. 7a) and monitor the end point levels (Fig. 7b). It was confirmed that the sensor surfaces were properly regenerated and the assay showed high reproducibility.

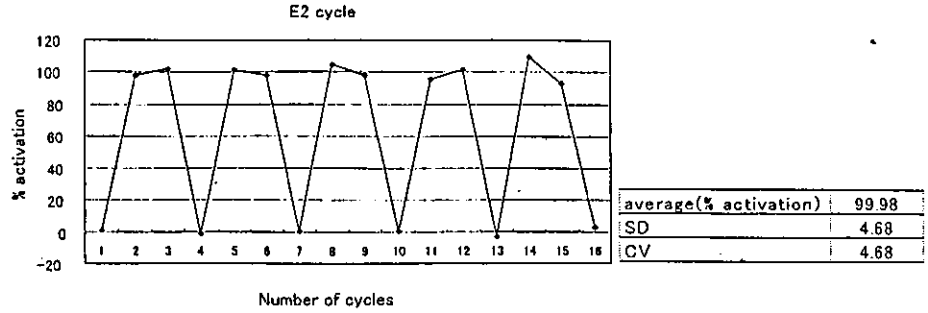

Fig. 8 Precision of the ER-ERE assay.

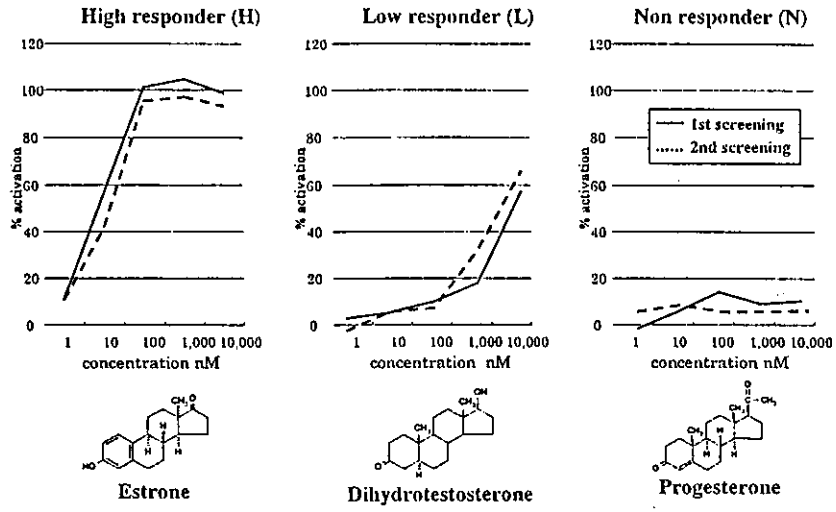

Fig. 9 Three types of chemical responses.

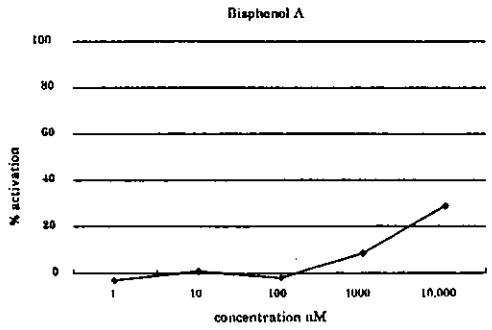

Fig. 10 Results of Bisphenol A.

The difference in the end point level was within 4 RU and the annealing level of anti-ERE was kept constant at around 25 RU throughout 30 cycles (Fig. 7c). We tested the reproducibility by repeating positive and negative controls for 16 cycles. It was shown that the results were with high precision with a CV% value of 4.68%, as shown in Fig. 8.

Screening results of 30 chemicals

We tested 30 chemicals to check the dose-dependent activation of the ER binding. One cycle of the assay took 15 min and the screening of one chemical was completed with 9 cycles in 2.5 h, including 5 different concentrations of the test chemicals, the positive and negative controls repeated twice for each control. We calculated the relative activation (% activation) using the formula shown in Fig. 4 for 30 chemicals. Based on the values of % activation at 100 nM of each chemical, chemicals could be classified into three groups (Fig. 9): the chemicals that showed more than 50% of the activation as "high responders", those with 20 - 50% as "low responders" and those less than 20% as "non-responders". The results obtained with two independent sets of screening were summarized in Table 1. 28 out of 30 chemicals showed the same results in the first and the second screening. 17β-Estradiol and its derivatives were classified to "high responders", while male hormones (progesterone) were "non-responders". Bisphenol A which is regarded as one of the endocrine disruptors, was classified among "low responders" (Fig. 10).

Furthermore, the differences in the effect of the chemicals on the ER binding activities were observed in the different shapes of the sensorgrams among those of 17β-estradiol, bisphenol A, 17α-estradiol, diethylstilbestrol (DES), tamoxifen and progesterone (Fig. 11). We have plotted the binding level at the end of the injection of ER in the presence of 1 μM of the test chemical (Y axis) *versus* the binding stability 2 min after the end of the ER injection (X axis), as shown in Fig. 12. We found that the agonists and the antagonists had significantly different patterns. The antagonists (such as tamoxifen) had a tendency to stabilize the binding of ER to ERE. The assay using Biacore indicated the possibility not only to detect the estrogenic activities of the chemicals, but to distinguish the antagonists from the agonists.

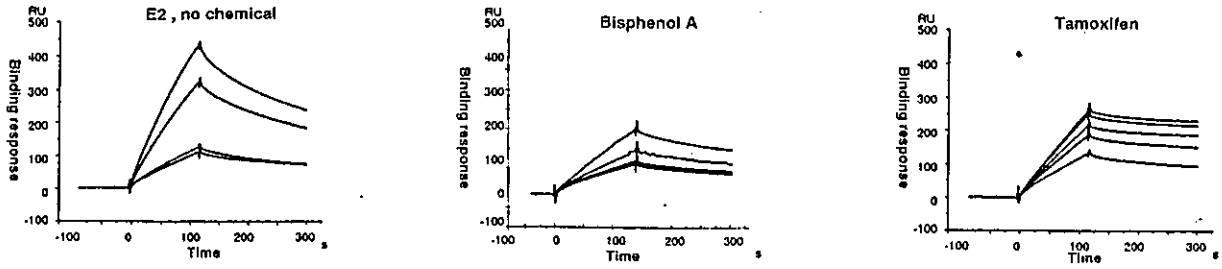

Fig. 11 Different kinetic patterns in the ER-ERE interaction.

Table 1 Results of ER-ERE screening with SPR sensor

No.	CAS No.	Name	1st Screening	2nd Screening
1	000050-28-2	Estradiol	H	H
2	000057-91-0	Estra-1,3,5(10)-triene-3,17-diol (17α)	H	H
3	000053-16-7	Estrone	H	H
4	000057-63-6	19-Nor-17-alpha-pregna-1,3,5(10)-trien-20-yne-3,17-diol	H	H
5	000362-05-0	Estra-1,3,5(10)-triene-2,3,17-beta-triol	H	H
6	000362-07-2	Estra-1,3,5(10)-triene-3,17-diol, 2-methoxy-, (17β)-	L	L
7	000068-22-4	19-Nor-17-alpha-pregn-4-en-20-yn-3-one, 17-hydroxy-	L	L
8	000063-05-8	Androst-4-ene-3,17-dione	N	N
9	000057-83-0	Progesterone	N	N
10	000501-24-6	3-Pentadecylphenol	N	N
11	005153-25-3	Benzoic acid, 4-hydroxy-, 2-ethylhexyl ester	N	L
12	001034-01-1	Gallic acid, octyl ester	N	N
13	006807-17-6	4,4'-(1,3-Dimethylbutylidene)bisphenol	L	L
14	027955-94-8	Phenol, 4,4',4"-ethylidynetri-	N	N
15	000081-92-5	Benzenemethanol, 2-[bis(4-hydroxyphenyl)methyl]-	L	L
16	000081-90-3	o-Toluic acid, .alpha.,.alpha.-bis(p-hydroxyphenyl)-	N	N
17	000978-86-9	4-(Triphenylmethyl)phenol	L	L
18	062625-31-4	Phenol, 4,4'-(3H-1,2-benzoxathiol-3-ylidene)bis 3-methyl-, S,S-dioxide, monosod	N	N
19	005384-21-4	Phenol, 4,4'-methylenebis[2,6-dimethyl-	L	L
20	005613-46-7	2,6-Xylenol, 4,4'-isopropylidenedi-	L	L
21	000084-16-2	Phenol, 4,4'-(1,2-diethylethylene)di-, meso-	H	H
22	000084-17-3	Phenol, 4,4'-(diethylideneethylene)di-	L	H
23	56-53-1	diethylstilbestrol	H	H
24	006893-02-3	Alanine, 3-(4-(4-hydroxy-3-iodophenoxy)-3,5-diiodophenyl)-, L-	N	N
25	000500-38-9	Nordihydroguaiaretic acid	N	N
26	023239-51-2	Benzyl alcohol, p-hydroxy-alpha-(1-((p-hydroxyphenethyl)amino)ethyl)-, hydrochlo	N	N
27	001050-28-8	L-Tyrosine, N-L-tyrosyl-	N	N
28	000145-50-6	1(4H)-Naphthalenone, 4- .alpha.-(4-hydroxy-1-naphthyl)benzylidene -	L	L
29	000446-72-0	Genistein	L	L
30	000080-05-7	Bisphenol A	L	L

H, High responder; L, low responder; N, non-responder.

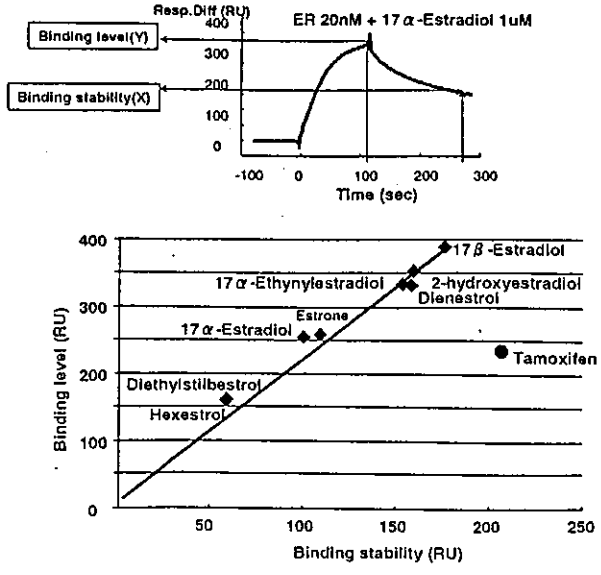

Fig. 12 Binding level *vs.* binding stability plot.

Discussion

We established a cell free screening method while focusing on the mechanism of the hormone receptor using a surface plasmon resonance sensor. We developed an assay method to detect estrogenic activities of the chemicals with changes in the binding level of ER to ERE by preincubating the chemicals with ER.

It was also suggested that the agonitst and the antagonists had different effects on the interaction of ER and ERE from an analysis of the binding level of ER during the association and dissociation processes. With the conventional end point assay used to monitor only the binding signals, it was impossible to distinguish the agonists from the antagonists. The real time analysis, which is the main feature of the surface plasmon resonance sensor enabled the classification of the agonists and the antagonists. When running the cell based hormone assay, it must be taken into account any unexpected effects of the chemicals to the other components than the receptors of the cells. On the other hand, the cell free assays simply show the

direct effects of chemicals to the receptor-signal transduction systems. Our new assay, based on the hormone receptor mechanism, can rapidly screen a large number of the chemicals for their hormonal activities.

Since other hormone receptors employ similar mechanism as ER for the activation of the gene expression, it is possible to develop same assays for other hormone receptors. A newly developed ER assay is both reliable and efficient as a primary screening method of chemicals for estrogenic activities.

Acknowledgements

This work was supported by Ministry of Health, Labour and Welfare of Japan.

References

1. "*White paper on the endocrine disrupting chemicals '99* (Japanese)", Environmental Agency, Japan, **1999**.
2. M. Nakai, Y. Tabita, D. Asai, Y. Yakabe, T. Shinmyozu, M. Noguchi, M. Takatsuki, and Y. Shimohigashi, *Biochem. Biophys. Res. Commun.*, **1999**, *254*, 311.
3. "*The interim report by the committee on the effects on health by the endocrine disrupting chemicals* (Japanese)", Ministry of Health and Welfare, Japan, **1998**.
4. A. M. Soto and C. Sonnenschein, *Biochem. Biophys. Res. Commun.*, **1984**, *122*, 1097.
5. M. Pons, D. Gagne, J. C. Nicolas, and M. Mehtali, *BioTechniques*, **1990**, *9*, 450.
6. J. R. Reel, I. V. J. C. Lamb, and B. H. Neal, *Appl. Toxicol.*, **1996**, *34*, 288.
7. OECD, OECD VALIDATION WORK ON IN-VIVO UTEROPHIC SCREENING ASSAY, **1999**.
8. "*Methods of the Biological Assays of the Endocrine Disrupting Chemicals*", ed. T. Inoue, **2000**, Springer Verlag, Tokyo.
9. P. Diel, T. Schulz, K. M. molnikar, E. Trunck, G. Ollmer, and H. Ichna, *J. Steroid Biochem. Mol. Biol.*, **2000**, *73(1 - 2)*, 1.
10. "*Real-Time Analysis of Biomolecular Interactions*", ed. K. Nagata and H. Handa, **1998**, Springer Verlag, Tokyo.
11. B. J. Cheskis, S. Karathanasis, and C. R. Lyttle, *J. Biol. Chem.*, **1997**, 272, 11384.

Available online at www.sciencedirect.com
SCIENCE DIRECT®
Toxicology 195 (2004) 19–29
TOXICOLOGY
www.elsevier.com/locate/toxicol

Exacerbation of benzene pneumotoxicity in connexin 32 knockout mice: enhanced proliferation of CYP2E1-immunoreactive alveolar epithelial cells

Byung-Il Yoon[a,b], Yoko Hirabayashi[a], Yasushi Kawasaki[a], Isao Tsuboi[a], Thomas Ott[c], Yukio Kodama[a], Jun Kanno[a], Dae-Yong Kim[b], Klaus Willecke[c], Tohru Inoue[a,*]

[a] *Division of Cellular and Molecular Toxicology, National Institute of Health Sciences, 1-18-1 Kamiyoga, Setagayaku, Tokyo 158-8501, Japan*
[b] *Department of Veterinary Pathology, College of Veterinary Medicine and Agricultural Biotechnology, Seoul National University, Seoul, Republic of Korea*
[c] *Institut für Genetik, Rheinische Friedrich-Wilhelms-Univesität, Bonn, Germany*

Received 3 March 2003; received in revised form 6 May 2003; accepted 25 August 2003

Abstract

The pulmonary pathogenesis triggered by benzene exposure was studied. Since the role of the connexin 32 (Cx32) gap junction protein in mouse pulmonary pathogenesis has been suggested, in the present study, we explored a possible role of Cx32 in benzene-induced pulmonary pathogenesis using the wild-type (WT) and Cx32 knockout (KO) mice. The mice were exposed to 300 ppm benzene by inhalation for 6 h per day, 5 days per week for a total of 26 weeks, and then sacrificed to evaluate the pneumotoxicity or allowed to live out their life span to evaluate the reversibility of the lesions and tumor incidence. Our results clearly revealed exacerbated pneumotoxicity in the benzene-exposed Cx32 KO mice, characterized by diffuse granulomatous interstitial pneumonia, markedly increased mucin secretion of bronchial/bronchiolar and alveolar epithelial cells, and hyperplastic alveolar epithelial cells positive for CYP2E1. But the results did not indicate any enhancement of pulmonary tumorigenesis in the Cx32 KO mice though the number of animals was small.

Keywords: Benzene; Connexin 32; Cx32 knockout mice; CYP2E1; Interstitial pneumonia; Pneumotoxicity

1. Introduction

Benzene has been reported to be a carcinogen capable of producing not only hemopoietic malignancies but also various solid tumors including lung cancers in mice, chronically exposed to it by ingestion or inhalation (Snyder et al., 1988; Huff et al., 1989; Farris et al., 1993).

Benzene toxicity and benzene-induced tumor development in the lung should be taken into consideration for the risk assessment in humans, since the lung is one of the benzene target organs and inhalation is the most common route through which humans are exposed to benzene. Furthermore, a strong relationship

* Corresponding author. Tel.: +81-3-3700-1564; fax: +81-3-3700-1622.
E-mail address: tohru@nihs.go.jp (T. Inoue).

0300-483X/$ – see front matter © 2003 Elsevier Ireland Ltd. All rights reserved.
doi:10.1016/j.tox.2003.08.014

between benzene exposure and lung cancer development in humans has been assumed for the past decades (Aksoy, 1985, 1989). In addition, benzene metabolites such as benzene oxide, benzene dihydrodiol and diolepoxide have been shown to induce lung tumorigenesis in mouse neonates (Busby et al., 1990). However, little information is available on the pulmonary pathogenesis triggered by benzene exposure.

Intercellular communication through gap junction proteins (GJICs) plays an important role in cellular homeostasis by regulating cell growth, cell differentiation, and apoptosis (Yamasaki, 1996). Based on this concept, alteration in GJICs has been demonstrated to be closely associated with the pathogenesis and carcinogenesis induced by chemicals, particularly by nongenotoxic agents (Yamasaki et al., 1995; Kolaja et al., 2000). Furthermore, down modulation of GJICs is known to induce cytochrome P450s by other chemicals that may be involved in benzene metabolism (Neveu et al., 1994; Snyder and Hedli, 1996; Shoda et al., 2000). We, therefore, hypothesized that GJICs may contribute also to the processes of benzene-induced pneumotoxicity and lung carcinogenesis.

As the presence and the functional role of connexin 32 (C32) gap junction protein in the mouse lung tissue have been suggested in previous in vitro and in vivo studies (Albright et al., 1990; Lee et al., 1997; Ruch et al., 1998; Abraham et al., 1999, 2001), in the present study, we explored a possible role of Cx32 in the lung pathogenesis induced by chronic exposure to benzene, using Cx32 knockout (KO) mice. For this purpose, wild-type (WT) and Cx32 KO mice were exposed to 300 ppm benzene by inhalation for 6 h per day, 5 days per week for 26 weeks. Then the pathological changes were determined based on the results of histopathology, histochemistry for detecting mucin secretion, and immunohistochemistry for detecting CYP2E1 and proliferating cell nuclear antigen (PCNA). The tumor incidence in the pulmonary tissue was also compared between the benzene-exposed WT and Cx32 KO mice.

2. Materials and methods

2.1. Animals

Cx32 KO mice, from the Institut für Genetik, Universität, Bonn, Germany (Moennikes et al., 2000), were maintained as heterozygous KO mice at the animal facility of National Institute of Health Sciences (NIHS), Japan. Because the *Cx32* gene is linked to the X-chromosome, we generated Cx32 WT ($Cx32^{+/Y}$) and KO male ($Cx32^{-/Y}$) mice for this study by cross breeding female $Cx32^{+/-}$ heterozygous mice and male C57BL/6 wild type mice. The Cx32 genotypes of the neonates were identified by the standard PCR assay (Moennikes et al., 2000). The WT and Cx32 KO mice aged 8–9 weeks were used in the study. During the study, the mice were housed within stainless-steel wire cages in inhalation chambers that were maintained on a 12-h light-dark cycle. The basal pellet diet (CRF-1; Funabashi Farm, Tokyo, Japan) was provided ad libitum, except during the 6-h daily inhalation of benzene when the food was withdrawn. Water was automatically supplied throughout the study.

2.2. Benzene exposure

Benzene was purchased from Wako Chemical Company (Osaka, Japan). The mice were randomized and exposed to benzene in 1.3 m^3 inhalation chambers, as described elsewhere (Yoon et al., 2001). Briefly, the benzene vapor was generated by heating liquid benzene to 16 °C and directed into the inhalation chambers (Sibata Scientific Technology Ltd., Tokyo, Japan) with a room temperature of 24 ± 1 °C. The flow rate of benzene was about 650 l/min, and the benzene concentration in the chambers was measured at 30-min intervals during the daily exposures using a gas chromatograph (Shimadzu Co., Kyoto, Japan). The temperature and humidity in the chambers were automatically controlled at 24 ± 1 °C and 55 ± 10%, respectively. As described in the previous Section 2.1, mice were supplied water ad libitum but withdrew the food pellets during the exposure.

The WT and Cx32 KO mice were, respectively, divided into the sham-exposed control group and the benzene-exposed groups; each group was composed of ten to twelve mice. The experimental group was exposed to 300 ppm benzene for 6 h per day, 5 days per week, for 26 weeks and the sham-exposed control group was maintained under the same conditions but without benzene inhalation. Five to six mice from each group were first sacrificed after the 26-week exposure to evaluate pneumotoxicity and the remaining five to seven mice from each group were allowed to

live out their lives to further evaluate their recovery from pulmonary lesions and the incidence of the pulmonary tumor.

2.3. Measurement of food consumption and body weight

Food consumption and body weight were measured every Friday throughout the 26-week benzene exposure.

2.4. Autopsy, organ weight measurement and histopathology

After the 26-week benzene exposure, five to six mice from each group were sacrificed under ethyl ether anesthesia for autopsy. Gross morphological examination of the mice was performed and the major visceral organs were weighed and analyzed. For the histopathological examination, tissues from both lungs were fixed in 10% neutral buffered formaldehyde for 24 h. Pulmonary tissues were sliced and immediately immersed in the fixative. After routine processing, the paraffin-embedded sections were stained with hematoxylin and eosin and then examined histopathologically under a light microscope.

2.5. Immunohistochemistry and histochemistry

The avidin–biotin–peroxidase complex (ABC) method was used for immunohistochemistry to detect the expression of the P450 CYP2E1 enzyme and PCNA. After the lung tissue sections mounted on poly-L-lysine-coated slides were deparaffinized and hydrated, endogenous peroxidase activity was blocked with methanol containing 0.3% hydrogen peroxide for 15 min. The lung tissue sections in a Caplin jar containing 1 mM citric acid (pH 6.0) were microwaved for 10 min for retrieval of PCNA. After washing in phosphate-buffered saline (PBS, pH 7.4) for 15 min, the tissue sections were incubated with 10% normal serum at room temperature for 60 min to block nonspecific binding sites. The sections were then incubated with a mouse anti-PCNA monoclonal antibody (1:300, Sigma–Aldrich, Amherst, NY, USA) for 50 min at room temperature and a goat anti-rat CYP2E1 polyclonal antibody (1:1000, Daiichi Pure Chemicals Co. Ltd., Tokyo, Japan) overnight at 4 °C. The tissue sections were washed three times in PBS, incubated with the corresponding biotinylated secondary antibodies for 40 min at room temperature, and subsequently incubated with the ABC reagent for 30 min at room temperature. As a chromogen, 0.5% 3,3′-diaminobenzidine tetrahydrochloride was used, and the sections were counterstained with methylene blue. As a positive control for PCNA and CYP2E1, normal testis and kidney sections were used, respectively, and as a negative control, PBS instead of the primary antibodies was applied to the sections.

Periodic acid–Schiff (PAS) reaction was performed to detect mucus secretion. After deparaffinization, the tissue sections were immersed in 0.5% periodic acid solution. After washing with distilled water, the sections were incubated with the Schiff reagent for 15 min, washed with warm tap water for 10 min, and then counterstained with hematoxylin.

2.6. Statistical analysis

ANOVA was performed to evaluate the significant differences in food consumption and body weight between the nonexposed sham exposed control and benzene-exposed groups of WT and Cx32 KO mice as well as between WT and Cx32 KO mice of each group.

3. Results

3.1. Changes in body weight during the 26-week benzene exposure

No significant difference was observed between WT and Cx32 KO mice of the nonexposed sham-control group throughout the study, even when the mean body weight of Cx32 KO mice was slightly less than that of WT mice at the late stage of this study (Fig. 1). Benzene exposure induced a significant decrease in the body weight of the benzene-exposed group of both WT and Cx32 KO mice compared with the nonexposed sham-control mice. The reduction was much more marked in Cx32 KO mice (Fig. 1), which was observed after seven weeks of exposure ($P < 0.05$). On the other hand, in WT mice, a significant difference in body weight was observed after the fourteenth week of exposure (Fig. 1). Furthermore, after the twelfth week

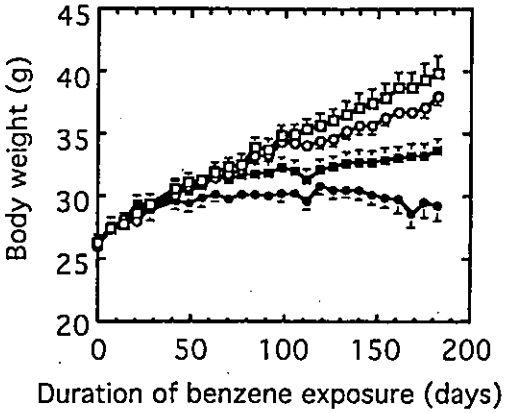

Fig. 1. Changes in body weights of WT and Cx32 KO mice during benzene exposure. Benzene (300 ppm) was inhaled for 6 h per day, 5 days per week for 26 weeks. Eleven to 12 mice per group were used. (□) WT-sham group; (○) Cx32 KO-sham group; (■) WT-benzene-exposed group; (●) Cx32KO-benzene-exposed group. There is significant difference between benzene-exposed group from the corresponding sham-control group after 10 weeks exposure for the Cx32 KO and 14 weeks exposure for WT. Vertical bars mean standard errors.

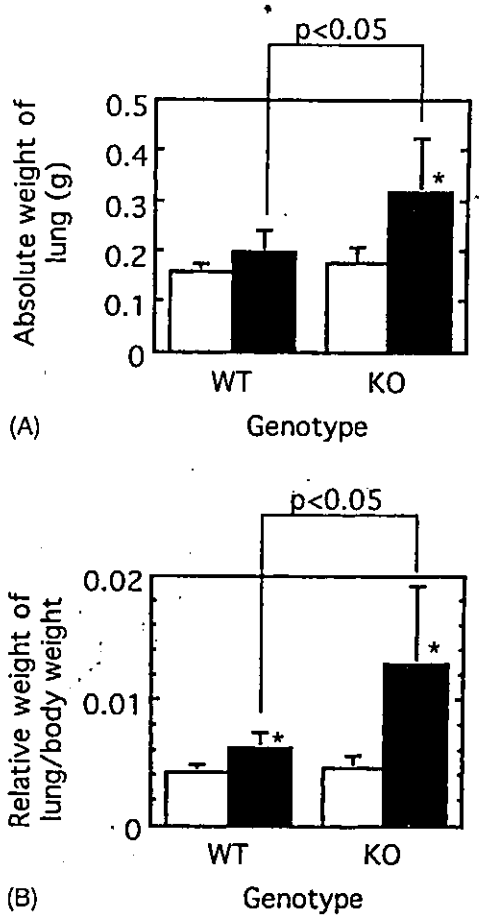

Fig. 2. Changes in weights of the lungs of mice exposed to 300 ppm benzene for 26 weeks. Open column; sham-control group, closed column; benzene-exposed group. Vertical bars mean standard deviations. Symbol (*) indicates significantly different from the corresponding sham-control group at $P < 0.05$.

of exposure, the mean body weight was significantly different between benzene-exposed WT and Cx32 KO mice ($P < 0.05$) (Fig. 1).

During the benzene exposure for 26 weeks, there had been no significant difference in food consumption between the nonexposed group and the benzene-exposed group of both WT and Cx32 KO mice and between WT and Cx32 KO mice of both groups (data not shown).

3.2. Weight of the lung

Significant increases were noted in the absolute lung weight of Cx32 KO mice and in the relative lung weights of both the WT ($P < 0.05$) and Cx32 KO mice ($P < 0.05$) after the twenty-sixth week of exposure to 300 ppm benzene (Fig. 2).

3.3. Histopathology and histochemistry

Severe diffuse interstitial pneumonia was observed in the lungs of the benzene-exposed Cx32 KO mice, which was comparable with that in the lungs of the WT mice showing much milder pulmonary lesions (Table 1, Fig. 3B and E). The alveolar walls were thickened by heavy infiltration of macrophages, the presence of a small number of lymphocytes and neutrophils, and a considerably increased number of type II alveolar epithelial cells (Fig. 3C). The proliferation of basophilic epithelial cells in the terminal bronchioles and alveolar ducts was frequently noted in the lungs of benzene-exposed Cx32 KO mice (Fig. 3F), while the lungs of benzene-exposed WT mice had mild and a few basophilic proliferating epithelial cell-proliferating foci. The numbers of mucus-secreting epithelial cells increased in the bronchi and bronchioli of both WT and Cx32 KO mice exposed to benzene for 26 weeks (Fig. 4C and D). In particular, in the benzene-exposed Cx32 KO mouse lungs, aggregates composed of mucin-secreting alveolar epithelial cells were occasionally detected (Fig. 4D).

Table 1
Pathological findings in the lungs of the wild-type (WT) and Cx32 knockout (KO) mice exposed to 300 ppm benzene for 26 weeks

Group (with or without benzene treatment)	Genotype			
	WT		Cx32 KO	
	Sham-exposed	300 ppm	Sham-exposed	300 ppm
Histopathology/no. of animals examined	6	5	5	5
Interstitial pneumonia granulomatous, diffuse	0 (0.0)	4 (80.0)	0 (0.0)	5 (100.0)
Moderate		4 (80.0)		1 (20.0)
Severe		0 (0.0)		4 (80.0)
Hyperplastic basophilic cell foci	0 (0.0)	1 (20.0)	0 (0.0)	4 (80.0)
Alveolar and bronchiolar epithelial cells		1 (20.0)		4 (80.0)
Mucin-secreting cells	0 (0.0)	5 (100.0)	1 (20.0)	5 (100.0)
Bronchial/bronchiolar epithelial cells		5 (100.0)	1 (20.0)	5 (100.0)
Alveolar epithelial cells		0 (0.0)	0 (0.0)	3 (60.0)

Number in parentheses represents the percentage (%) of the lesions.

3.4. Immunohistochemistry for PCNA and CYP2E1

The labeling indices for PCNA, compared with those of the corresponding control groups, significantly increased in both benzene-exposed WT and Cx32 KO mice; from 79.9 to 162.3‰ ($P < 0.005$) and 92.7 to 533.0‰ ($P < 0.002$), respectively (Fig. 5).

A few bronchial and bronchiolar epithelial cells of sham-control WT and Cx32 KO mice were positive for the CYP2E1 enzyme (Fig. 6A). The numbers of

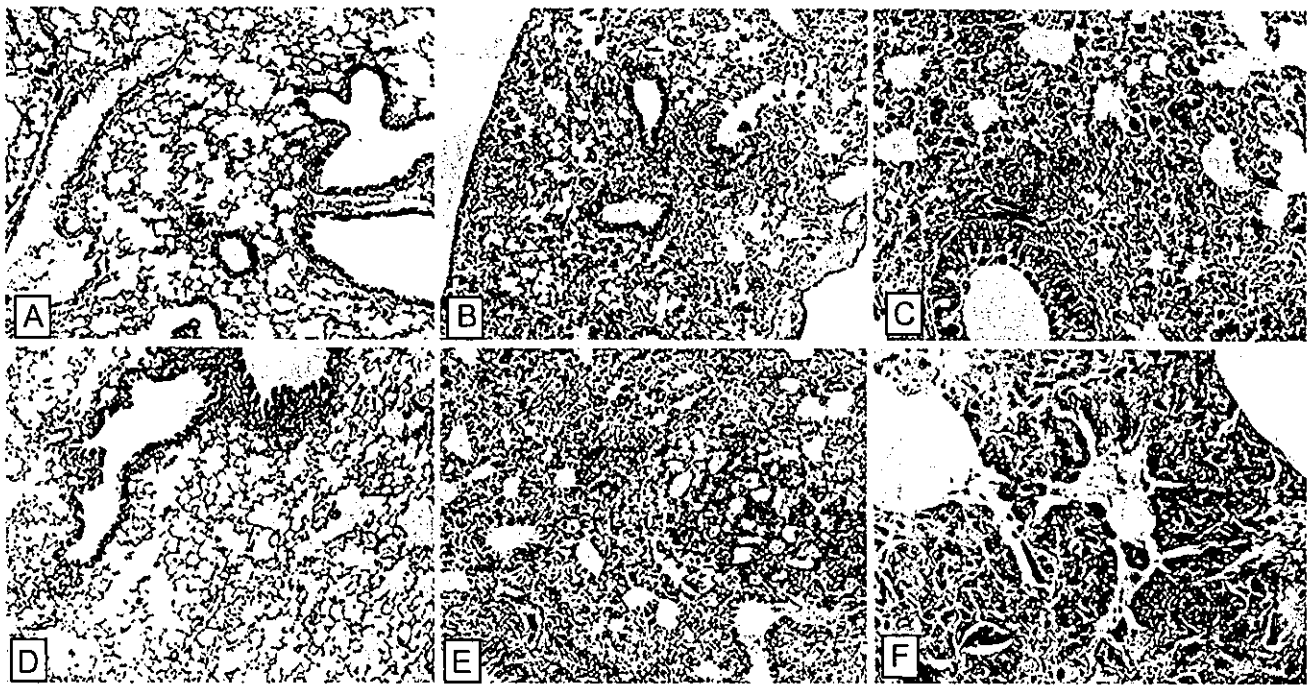

Fig. 3. Histopathological changes of the lungs of benzene-exposed WT and Cx32 KO mice exposed to 300 ppm benzene for 26 weeks. (A) sham-control WT mice, (B and C) benzene-exposed WT mice, (D) sham-control Cx32 KO mice, (E and F) benzene-exposed Cx32 KO mice. Note the granulomatous interstitial pneumonia in the lungs of benzene-exposed WT and Cx32 KO mice, and basophilic epithelial cell-proliferating foci frequently observed in the lungs of benzene-exposed Cx32 KO mice (F). Original magnification: (A) ×100; (B) ×100; (C) ×200; (D) ×100; (E) ×100; (F) ×400. Hematoxylin- and eosin-stained.

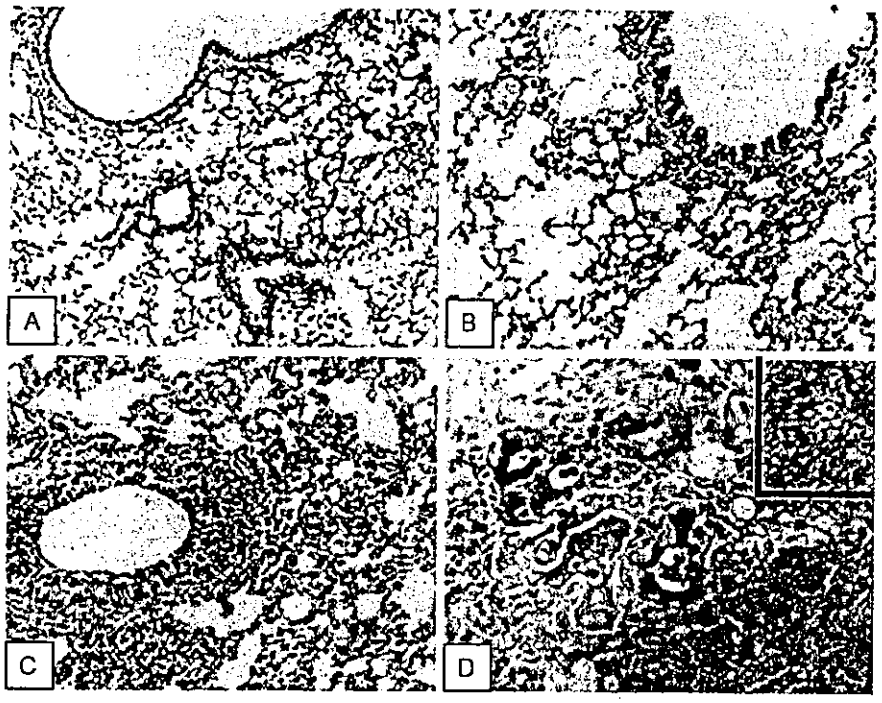

Fig. 4. Histochemistry for detection mucin secretion. (A) Sham-control WT mice, (B) sham-control Cx32 KO mice, (C) benzene-exposed WT mice, (D) benzene-exposed Cx32 KO mice. Note the enhanced mucin secretion from bronchiolar epithelial cells of WT mice (C) and Cx32 KO mice (Inset in D), and the aggregated cells releasing mucin occasionally observed in the benzene-exposed Cx32 KO mice (D). Original magnification: (A) ×200; (B) ×200; (C) ×200; (D) ×400.

CYP2E1-positive bronchial and bronchiolar epithelial cells considerably increased following long-term benzene exposure in both WT and Cx32 KO mice (Fig. 6B). The proliferating basophilic alveolar epithelial cells frequently observed in the benzene-exposed Cx32 KO mice were strongly positive for CYP2E1 (Fig. 6D), which was significantly comparable with the WT mice in which these findings were rarely observed.

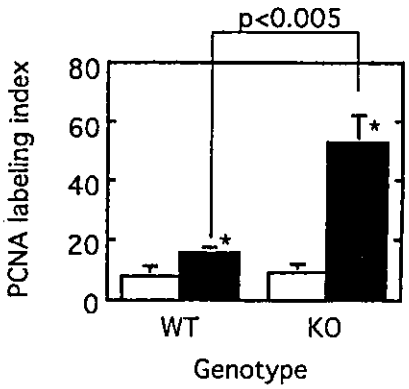

Fig. 5. PCNA labeling indices in the mouse lung tissues exposed to 300 ppm benzene for 26 weeks. Values represent the number of PCNA-positive cell per 1000 cells. More than 3,000 alveolar epithelial cells were counted under a light microscope at a high magnification (×400).

3.5. Survival curves for life time observation

Five to seven mice were randomly selected and allowed to live their life span to evaluate their recovery from pulmonary lesions and the incidence of pulmonary tumor. Survival curves for each group are shown in Fig. 7. In each group the number of mice were limited to about five to seven mice per group. There was no intermittent death during the exposure time up to 182 days (26 weeks). The sham-exposed control group indicated by open symbols, circles for WT mice and squares for Cx32 KO mice, show a longer life span than the benzene-exposed group indicated by closed symbols, circles for WT mice and squares for Cx32 KO mice. Interestingly, in the exposed group, Cx32 KO mice showed a longer life span than the wild-type mice, although the sham-exposed group does not show much difference between wild-type mice and Cx32 KO mice. During the observation period, all the mice that